Magnetic Thermoresponsive Core−Shell Nanoparticles

Thorsten Gelbrich, Mathias Feyen, and Annette M. Schmidt*

Institute for Organic Chemistry and Makromolecular Chemistry II, Heinrich Heine University of Düsseldorf, Universitätsstr. 1, D-40225 Düsseldorf, Germany

Received January 2, 2006
Revised Manuscript Received February 17, 2006

Introduction

Magnetic fluids[1] achieve growing attraction from the biosciences due to numerous present and future applications[2] including in vitro automated separation and isolation of biomolecules and cells.[3] These dispersions of magnetic nanoparticles are attractive in separation applications as they offer high surface area and can be functionalized to selectively discriminate between different molecular or cellular species. Present suggestions for nonmedical applications of magnetic fluids include the use of magnetic fluids as magnetically separable nanocatalytic systems that combine the advantages of homogeneous and heterogeneous catalysis.[4] For this purpose, immobilizing sites for catalytically active species like metal complexes or enzymes are included to the stabilizing shell. In these applications, a small particle size and effective dispersion stability by a suitable stabilization mechanism are requested in order to achieve an optimum of specific binding or catalytic activity. In the same direction, however, these parameters complicate the magnetic separation of the particles.

A new strategy to meet this challenge is a thermoreversible stabilization of magnetic particles by the use of a well-defined polymeric shell with a critical solution behavior in the carrier fluid. Thermoreversible stabilization of the particles offers an opportunity to combine dispersibility and quasi-homogeneous conditions for specific binding and catalytic activity and easy magnetic separation at temperatures beyond the stabilizing conditions.

We present the first results on the synthesis and characterization of novel thermoreversible magnetic fluids based on magnetite (Fe_3O_4) coated with a covalently anchored, polymeric shell of poly(2-methoxyethyl methacrylate) (PMEMA). The core−shell particles form stable dispersions in methanol at temperatures above an upper critical solution temperature (UCST), while the particles precipitate below that temperature and can easily be separated by a magnet.

Results and Discussion

The synthetic pathway is composed of alkaline precipitation of magnetite nanoparticles,[5] followed by surface functionalization of the particles and surface initiated atom transfer radical polymerization (ATRP), as outlined in Scheme 1. ATRP is a preferred "grafting-from" method in surface-initiated polymerization from colloidal particles,[6] as it offers the advantage of a "living"/controlled mechanism leading to linear chains with low polydispersity and good control on the molecular weight and a fairly good resistance to additional reaction components and impurities. It therefore shows the preconditions required to create a well-defined polymeric shell with linear arms of high grafting density, referred to as a polymeric brush.[7]

Scheme 1. Synthesis of Fe_3O_4@PMEMA Hybrid Nanoparticles by Surface-Initiated ATRP

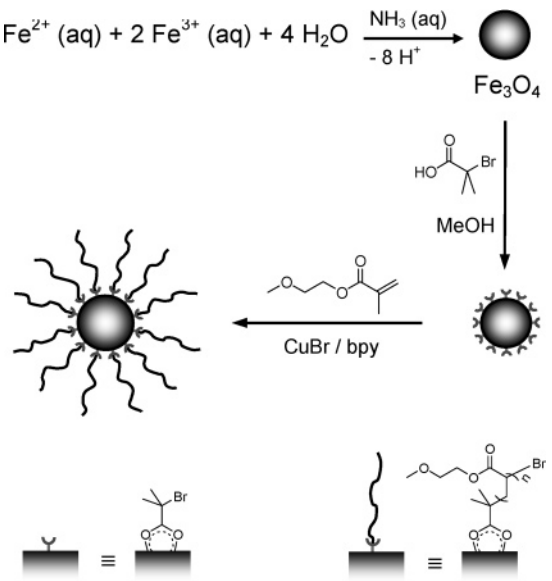

Alkaline precipitation of the magnetic cores leads to magnetite (Fe_3O_4) nanoparticles confirmed by X-ray diffractometry (XRD, see Supporting Information). The volume average core sizes calculated from XRD by the Scherrer method[8] (11.8 nm) and from VSM of hybrid particle dispersions (Table 1) are in good agreement. The size distribution of the particles can be detected from TEM images (Figure 1b) and gives a number-average core diameter of 10.1 nm.

The functionalization of freshly precipitated magnetite (Fe_3O_4) nanoparticles by chemisorption of 2-bromo-2-methylpropionic acid (BIB) can be verified by ATR−IR spectroscopy[9] (see Experimental Section) and quantified by thermogravimetric analysis (TGA) and elemental analysis (EA). We find an initiator density f_{ini} of 0.33 mmol (EA) per gram of Fe_3O_4 and 0.26 mmol g^{-1} (TGA).

Hybrid particles were obtained by surface-initiated ATRP of MEMA catalyzed by a copper(I) bromide/2,2′-bipyridine (bpy) system. Washed and dried samples were analyzed by ATR−IR (see Experimental Section) and TGA. From TGA experiments, a magnetite mass content between 16 and 43 mass % is extracted.

TEM images of Fe_3O_4@PMEMA*18* casted from DMF confirm the architecture of the hybrid particles (Figure 1). Strongly contrasting, nearly spherical magnetite cores can be clearly distinguished from a closed polymeric shell. Within the observed small particle aggregates that are possibly formed during sampling, the single magnetite cores are mostly visibly separated by a PMEMA shell. We estimate a polymer layer thickness of 3−5 nm, independent of the individual core size.

A brief characterization of the polymeric shell is possible after dissolution of the magnetic cores by acidolysis with hydrochloric acid and isolation of the polymeric component by precipitation. GPC analysis results in the calculation of number-average molecular weights M_n of the polymeric arms between 11 000 and 35 100 g mol^{-1} with a linear relation between μ_{PMEMA}/μ_M and M_n,[10] leading to a calculated chain density f_s of

* Corresponding author: e-mail schmidt.annette@uni-duesseldorf.de; phone +49-211-8114820; fax +49-211-8115840.

10.1021/ma060006u CCC: $33.50
Published on Web 04/05/2006

Table 1. Composition of Investigated Fe_3O_4@PMEMA Core−Shell Nanoparticles[a]

sample[b]	μ_M[c] (%)	d_c[d] (nm)	M_n[e] (g mol^{-1})	M_w/M_n[e]	μ_{MF}[f] %	d_h[g] (nm)
Fe_3O_4@PMEMA*43*	43	11.8	11 000	1.85	2.9	30 ± 3
Fe_3O_4@PMEMA*30*	30	12.9	16 800	3.09	1.0	47 ± 3
Fe_3O_4@PMEMA*18*	18	n.d.	30 900	2.16	n.d.	55 ± 5
Fe_3O_4@PMEMA*16*	16	12.2	35 100	2.15	0.48	73 ± 7

[a] μ_M = mass content of Fe_3O_4 in dry particles, d_c = core diameter, M_n = number-average molecular weight of polymeric arms, M_w/M_n = polydispersity index, and μ_{MF} = mass content of Fe_3O_4 in saturated DMF dispersions. [b] Sample denotations: Fe_3O_4@PMEMA μ_M. [c] TGA results. [d] Calculated from initial susceptibility (VSM). [e] GPC results relative to PS and corrected by the Mark−Howink relationship. [f] Calculated from saturation magnetization (VSM). [g] DLS results. n.d. = not determined.

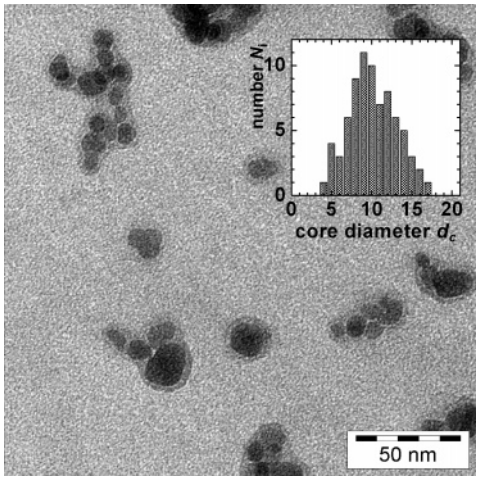

Figure 1. TEM image of Fe_3O_4@PMEMA*18* hybrid particles. Inset: core size distribution (TEM, n = 76).

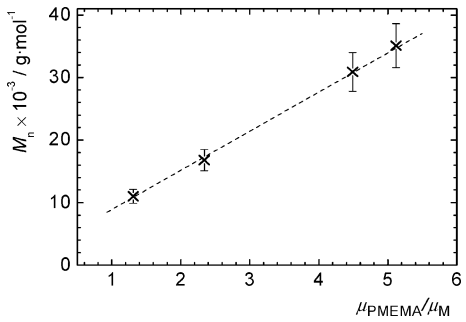

Figure 2. Molecular weight M_n vs mass ratio μ_{PMEMA}/μ_M (TGA) of dry Fe_3O_4@PMEMA particles (μ_{PMEMA} = 100% − μ_M). The slope gives the chain density f_s per gram of Fe_3O_4.

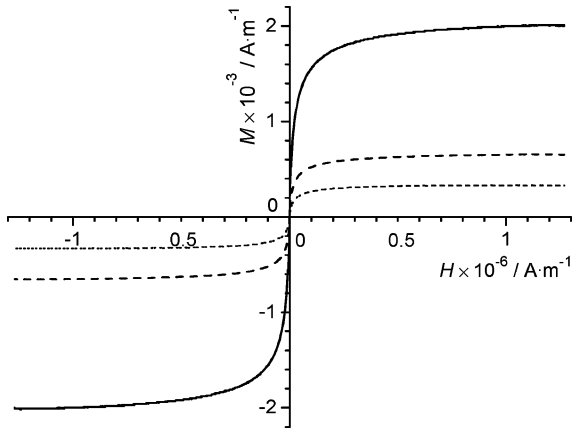

Figure 3. VSM loops of saturated magnetic fluids based on Fe_3O_4@PMEMA nanoparticles in DMF: compact line, Fe_3O_4@PMEMA*43*; dashed line, Fe_3O_4@PMEMA*30*; dotted line, Fe_3O_4@PMEMA*16*.

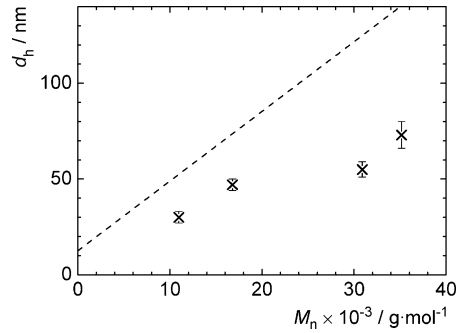

Figure 4. Hydrodynamic peak diameter d_h (DLS) vs molecular weight M_n (GPC) for Fe_3O_4@PMEMA particles. The dotted line represents the contour length of stetched polymer chains.

0.16 mmol per gram of Fe_3O_4 (Figure 2), a value that is lower than the initiator functionality f_{ini} from TGA and EA. The polydispersity indices are found to be around 2, except a value of 3 for sample Fe_3O_4@PMEMA*30* (Table 1). The comparably broad molecular weight distribution for ATRP products can be attributed to termination reactions supposed to occur primarily at the beginning of the polymerization. At that time the initial number of radicals generated on the particle surface by bromine transfer to Cu(I) is high compared to the concentration of deactivating Cu(II) species in solution. As a result, the deactivation of the radicals is supposed to be too slow to effectively suppress chain termination by coupling or disproportional reactions.[11]

The polymeric shell is predominantly responsible for the dispersibility of the obtained hybrid particles in suitable solvents. We find that freshly prepared PMEMA-capped magnetite nanoparticles instantaneously form stable dispersions (magnetic fluids) in *N*,*N*-dimethylformamide (DMF) with up to 2.9 mass % of magnetite, which remain stable for months and show a good stability toward dilution.

The dispersions show superparamagnetic behavior in VSM experiments with low coercitivity values (<0.6 kA m^{-1}) (Figure 3).[12] The saturation magnetization and initial susceptibility obtained from the experiments give information on the magnetite content and the volume average magnetite core size (see Table 1). The good agreement with the core diameter as observed in TEM indicates that the particle cores respond individually to the magnetic field.

In DLS experiments, we observed an increase of the hydrodynamic diameter d_h of Fe_3O_4@PMEMA hybrid particles dispersed in DMF with the polymeric arm length given by M_n by DLS (Figure 4). Compared to the theoretical relationship given by the simple model of ideally stretched polymer chains (dotted line in Figure 4), the obtained hydrodynamic diameters derivate up to 50% to lower values, with a higher deviation for higher M_n. This indicates that the results are within the expected dimension for single particles carrying a polymeric brush of extended chains in a condition between coiled and fully stretched.[7]

Thermoreversible magnetic fluids are obtained by dispersing Fe_3O_4@PMEMA particles in methanol. Below a critical temperature T_{crit} (UCST behavior) that depends on the polymer arm length, the particles show poor dispersibility and precipitate

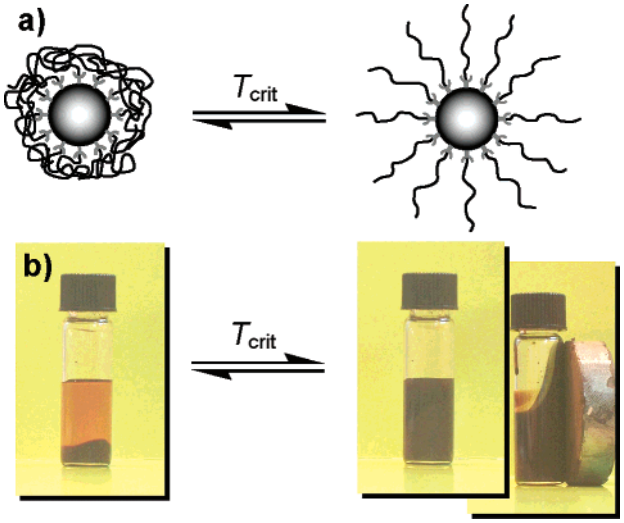

Figure 5. (a) Schematic behavior of the polymer brush shell in thermoreversible magnetic fluids. (b) Photographs of Fe_3O_4@PMEMA*43* in DMF. The particles precipitate below T_c (at 20 °C, left-hand). A particle dispersion is formed above T_c (at 50 °C, right-hand) that reacts collectively under the influence of a permanent magnet.

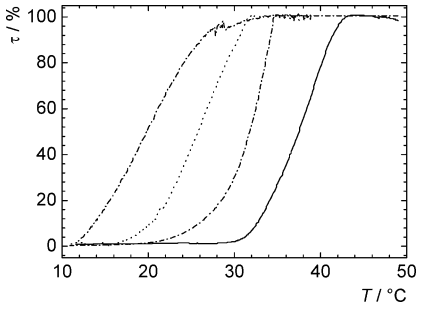

Figure 6. Relative transmittance τ vs temperature T of Fe_3O_4@PMEMA suspensions in methanol in turbidity experiments: compact line, Fe_3O_4@PMEMA*43*; dashed line, Fe_3O_4@PMEMA*30*; dotted line, Fe_3O_4@PMEMA*18*; dash−dotted line, Fe_3O_4@PMEMA*16*.

almost readily, while heating above T_{crit} results in solvation of the polymeric shell (Figure 5a). Consequently, the hybrid particles form a stable dispersion that shows the typical behavior of a magnetic fluid including collective response to a permanent magnet (Figure 5b).

Turbidity experiments (Figure 6) of dilute suspensions indicate a sudden increase of the optical transmittance with increasing temperature while the turbid suspension is converted to a brownish transparent dispersion. Surprisingly, the experiments indicate that the cloud point (defined by the inflection point of the graphs) is lower in dispersions of particles with longer polymer arms, oppositional to what would have been expected. One possible explanation is the surface attachment of the arms, leading to crowded and therefore more or less stretched polymer chains. For this reason the entropic contribution to the solvation process is less beneficial than for free polymer chains. It is expected that this effect is less relevant for long chains, as the free volume of chain segments increases with rising distance to the solid core. In contrast to the hybrid particles, free PMEMA model polymers show good solubility in methanol in the observed range of concentration and temperature.

In summary, we have described the synthesis of nanoscopic magnetite-cored polymeric brushes by surface-initiated ATRP and the properties of novel thermoreversible magnetic fluids based thereon. The presented combination of thermoresponsive polymers with the properties of magnetic fluids, together with tailorable hydrodynamic diameter and critical temperature, contributes to the development of easily recoverable polymer-supported magnetic separation kits and catalytic systems.

Experimental Section

Analytical Methods and Instrumentation. Elemental analysis (EA) was performed on a Perkin-Elmer 2400 (series 2) CHN analyzer. The functionalization density was calculated on behalf of the C content. ATR−IR spectra were recorded on a Nicolet FT-IR-5SXB spectrometer. For the TGA a Netsch STA 449c in a He atmosphere was used with a heating rate of 10 K min^{-1} between 30 and 600 °C. Weight loss of dry functionalized or hybrid particles between 200 and 410 °C was attributed to the content of BIB or PMEMA, respectively. Gel permeation chromatography (GPC) elugrams were collected in THF (300 × 8 mm^2 MZ Gel SDplus columns, Waters 410 RI-detector) relative to polystyrene standards. Results were corrected by the Mark−Houwink relationship.[13] Vibrating sample quasi-static magnetometry (VSM) was performed on a MicroMag vibrating sample magnetometer from Princeton Measurements Corp. with a field maximum of 1.3×10^6 A m^{-1}. DLS experiments were implemented on a Malvern HPPS-ET at 25 °C. TEM pictures were taken on a Zeiss (LEO) 912 Omega (120 kV) on DMF-casted samples. Turbidity experiments were recorded on a Tepper cloud point photometer.

BIB-Functionalized Fe_3O_4 Nanoparticles. Alkaline precipitation of magnetite nanoparticles was conducted on the basis of the method of Massart and Cabuil.[5] The aqueous suspension was washed several times with 1.3 vol % ammonium hydroxide solution and methanol. The fresh particle suspension was stirred with 1.67 mmol (277.2 mg) of BIB per gram of magnetite for 30 min, and the particles were washed extensively with methanol.

ATR−IR spectra of dried functionalized Fe_3O_4 nanoparticles show several characteristic peaks in the fingerprint region (ν = 1465, 1402, 1375, and 1107 cm^{-1}) also found in ATR−IR spectra of the free acid. The vibrational absorption of the carbonyl double bond (ν = 1548 cm^{-1}) shows a shift and a dramatic decrease in intensity in comparison to the free BIB (ν = 1702 cm^{-1}) while the deformational stretching absorption of the (CO)−O−H group (ν = 1292 cm^{-1}) vanishes, attributed to the chemisorption via the carboxylate group.[8]

Fe_3O_4@PMEMA Core−Shell Nanoparticles. Fe_3O_4@PMEMA hybrid particles were obtained by adding CuBr and bpy (1:2.5 mol/mol) in methanol to the particle suspension in MEMA and stirring at ambient temperature for 48 h. The formed core−shell nanoparticles were dispersed either in DMF or in warm methanol (50 °C). Acidolysis of the magnetite cores occurs by treating the DMF-based magnetic fluids with concentrated hydrochloric acid. Afterward, the polymer component is precipitated in water. Common ATR−IR peaks of dried Fe_3O_4@PMEMA particles with PMEMA model polymers are found at e.g. ν = 1722, 1241, 1151, 1123, and 865 cm^{-1}.

Acknowledgment. We thank Prof. Dr. H. Ritter for his steady interest and continuous support of this work and Prof. Dr. W. Frank, HHU Düsseldorf, for TGA experiments, Prof. Dr. W. Gawalek, IPHT Jena, for VSM, and Dr. S. Santer, IMTEK Freiburg, for TEM images. A.S. thanks the Fonds der Chemischen Industrie for a Liebig grant. This work is supported by the DFG (SPP1104).

Supporting Information Available: X-ray diffractogram of bare magnetite nanoparticles. This material is available free of charge via the Internet at http://pubs.acs.org.

References and Notes

(1) (a) Berkovsky, B. M.; Bashtovoy, V. *Magnetic Fluids and Applications Handbook*; Begell House: New York, 1996. (b) Blums, E.; Cebers, A.; Mairov, M. M. *Magnetic Fluids*; Walter de Gruyter: Berlin, 1997.

(2) (a) *Magnetism in Medicine*; Andrä, W., Nowak, H., Eds.; Wiley-VCH: Berlin, 1998. (b) Pankhurst, Q. A.; Connolly, J.; Jones, S. K.; Dobson, J. *J. Phys. D: Appl. Phys.* **2003**, *36*, R167−R181. (c) Tartaj, P.; Morales, M. P.; Veintemillas-Verdaguer, S.; Gonzáles-Carreno, T.; Serna, C. J. *J. Phys. D: Appl. Phys.* **2003**, *36*, R182−R197. (d) Berry, C. C.; Curtis, A. S. G. *J. Phys. D: Appl. Phys.* **2003**, *36*, R198−R181.

(3) (a) Gu, H.; Ho, P. L.; Tsang, K. W. T.; Wang, L.; Xu, B. *J. Am. Chem. Soc.* **2003**, *125*, 15702. (b) Patolsky, F.; Weizmann, Y.; Kratz, E.; Willner, I. *Angew. Chem.* **2003**, *115*, 2474−2478; *Angew. Chem., Int. Ed.* **2003**, *42*, 2372. (c) Nam, J. M.; Thaxton, C. S.; Mirkin, C. A. *Science* **2003**, *301*, 1884.

(4) (a) Lu, A. H.; Schmidt, W.; Matoussevitch, N.; Bönnemann, H.; Spliethoff, B.; Tesche, B.; Bill, E.; Kiefer, W.; Schüth, F. *Angew. Chem.* **2004**, *116*, 4403−4406; *Angew. Chem.* **2004**, *43*, 4303−4306. (b) Teunissen, W.; de Groot, F. M. F.; Geus, J.; Stephan, O.; Tence, M.; Colliex, C. *J. Catal.* **2001**, *204*, 169−174.

(5) Massart, R.; Cabuil, V. *J. Chem. Phys.* **1987**, *84*, 967−973.

(6) (a) von Werne, T.; Patten, T. E. *J. Am. Chem. Soc.* **2001**, *123*, 7497−7505. (b) Ohno, K.; Koh, K.; Tsujii, Y.; Fukuda, T. *Angew. Chem.* **2003**, *115*, 2857−2860; *Angew. Chem., Int. Ed.* **2003**, *42*, 2751−2754. (c) Duan, H.; Kuang, M.; Wang, D.; Kurth, D. G.; Möhwald, H. *Angew. Chem.* **2005**, *117*, 1745−1748; *Angew. Chem., Int. Ed.* **2005**, *44*, 1717−1720. (d) Chen, X.; Randall, D. P.; Perruchot, C.; Watts, J. F.; Patten, T. E.; von Werne, T.; Armes, S. P. *J. Colloid Interface Sci.* **2003**, *257*, 56−64.

(7) *Polymer Brushes*; Advincula, R. C., Brittain, W. J., Caster, K. C., Rühe, J., Eds.; Wiley-VCH: Weinheim, 2004.

(8) Scherrer, P. *Nachr. Ges. Wiss. Göttingen* **1918**, *Math.-Phys. Kl. 2*, 98.

(9) Rocchiccioli-Deltcheff, C.; Franck, R.; Cabuil, V.; Massart, R. *J. Chem. Res.* **1987**, 1209−1230.

(10) (a) Schmidt, A. M. *Macromol. Rapid Commun.* **2005**, *26*, 93−97. (b) Schmidt, A. M. *J. Magn. Magn. Mater.* **2005**, *289C*, 5−8.

(11) Matyjaszewski, K.; Davis, T. P. *Handbook of Radical Polymerization*; Wiley-Interscience: New York, 2002.

(12) Rosensweig, R. E. *Ferrohydrodynamics*, 1st ed.; Cambridge University Press: New York, 1985.

(13) Schindler, A.; Hibionada, Y. M.; Pitt, C. G. *J. Polym. Sci., Polym. Chem. Ed.* **1982**, *20*, 319.

MA060006U